Optical and Mechanical Response of High Temperature Optical Fiber Sensors

by

Jim Sirkis
Assistant Professor
Department of Mechanical Engineering
University of Maryland
College Park, Maryland 20742

The National Aerospace Plane (NASP) will experience temperatures as high as 2500 F at critical locations in its structure. Optical fiber sensors have been proposed as a means of monitoring the temperature in these critical regions by either bonding the optical fiber to, or embedding the optical fiber in, metal matrix composite components (MMC). Unfortunately the anticipated NASP temperature ranges exceed the glass transition region of the optical fiber glass. This study attempts to define the operating temperature range of optical fiber sensors from both optical and mechanical perspectives. The two underlying questions which are addressed ar "What are we measuring?" and "Will the fiber, bonding agent, and/or MMC survive the thermomechanical loading?" Both of these are issues define the usefulness of glass optical fibers for high temperature measurements. Glass transition is the phenomena where the material properties of the optical fiber drastically change during a well define temperature range (roughly 900 F to 1100 F). Properties such as coefficient of thermal expansion, Young's modulus, Poisson's ratio, fracture toughness, and refractive index can all change by as much as a order of magnitude. The behavior of these properties is a non-linear function of time and temperature, and as a result is highly dependent on the time-temperature history. A full non-linear optical analysis has been performed by modeling the optical response of an isolated sensor cyclically driven through the glass transition region. The mechanical analysis addresses the mechanical reliability of an optical fiber embedded in a transversely isotropic MMC. This analysis included non-linearities with temperature, but not with time.

Optical Response

The response of the optical phase lock loop (OPLL) sensor proposed by NASA LaRC for NASP applications is governed by optical path length. Optical path length is proportional to the refractive index and total length of the optical fiber. Under uniform thermal loading, the total length is governed by thermal expansion. The refractive index and thermal expansion can both be modeled

through glass transition using Narayanaswamy's [1] method of defining a reduced time and thermorheological simplicity. The parameters which govern this model for thermal expansion and refractive index are available in the literature for borosilicate glass [2,3], which is similar to the glass compositions used in optical fibers. Figures 1b through 1d show the response of the thermal expansion, refractive index, and optical signal to the temperature history shown in Fig. 1a. The competing hysteresis in the thermal expansion and refractive index results in a reduced hysteresis in the optical signal. The optical signal response to a symmetric, three cycle, saw-tooth temperature history is shown in Fig. 2 where the hysteresis has collapsed onto a closed curve. This collapse is important since it indicates that the "calibration" of the optical fiber sensor will settle into a repeatable function of time.

Mechanical Response

The mechanical response of an optical fiber sensor/MMC system is analyzed for the case of an uncoated optical fiber embedded in a transversely isotropic host, and subjected to a uniform temperature distribution. The possible failure mechanisms which are explored are brittle fraction of the fiber, and failure of host MMC. Time did not permit a full history dependent non-linear analysis of the optical fiber mechanics, so only a temperature dependent non-linear analysis is described. The thermomechanical properties of the fiber and MMC show strong temperature dependence. Figure 3, for example, shows the temperature dependence of Young's modulus, shear modulus, and fracture toughness for float glass [4]. Notice the abrupt change in the character of all of these curves as the glass transition region is breached. This analysis assumes the system is in a state of generalized plane strain. The resulting axial stresses in the fiber are used as the far field stresses in a classical fracture mechanics analysis. The fiber is assumed to have a circumferential crack whose depth is typical of the flaw sizes sighted in the optical fiber literature. The radial stresses on the fiber are not included in the fracture analysis since they are non-singular. Sih's strain energy density criterion [5] is adopted since this method is purported to be applicable to brittle, ductile, and fully non-linear materials and loading. These characteristics are desirable since the optical fiber is expected to transition form brittle to ductile failure as the temperature is increased. The host MMC is transversely isotropic with different tensile and compressive strength characteristics. The Tsai-Wu failure model [6] is adopted for this material.

The stresses in the matrix are determined in the generalized plane strain analysis, and are highest at the interface with the optical fiber. The region of stress concentration is localized within five fiber diameters of the optical fiber center. Figure 4 shows the failure criterion for the fiber and the fiber/host interface plotted as a function of the applied temperature field. Failure is

predicted in the fiber when Sih's strain energy density ratio, S/Sc, exceeds 1, and likewise in the MMC when the Tsai-Wu failure function, F, exceeds 1. Failure is predicted in the fiber around 800 F and in the MMC at around 1150 F. The nonlinearity in S/Sc for the fiber is due to the competing temperature response of the material properties.

[1] Narayanaswamy, O. S, Jou. Am. Cer. Soc., 54 (10), pp. 491-498, 1971.
[2] Spinner, S., et al, Jou. Res. Nat. Bur. Std., 70A (2), pp. 147-152, 1966.
[3] Scherer, G. W., Relaxation in Glass and Composites, Wiley, NY, 1986.
[4] Shinkai, N., et al., Jou. Am. Cer. Soc., 64 (7), pp. 426-430, 1971.
[5] Sih, G. C., Eng. Fract. Mechs., 5, pp. 1037-1040, 1973.
[6] Tsai, S. W., and Wu, E. M, Jou. Comp. Mat., 5, pp. 58-80, 1971.

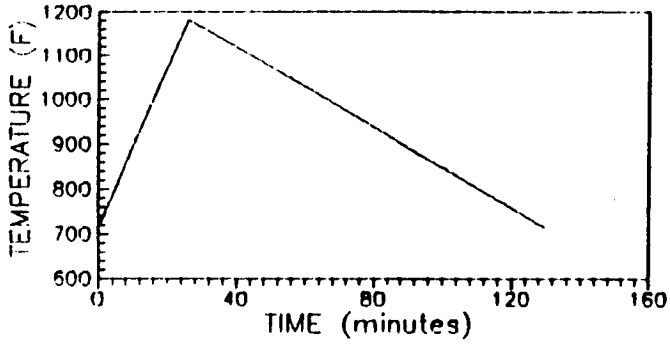

Figure 1a.

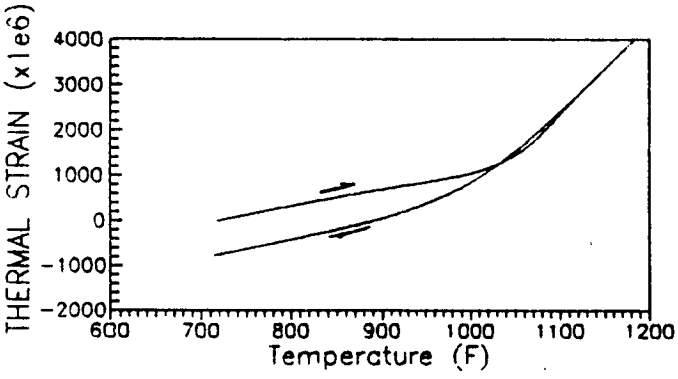

Figure 1b.

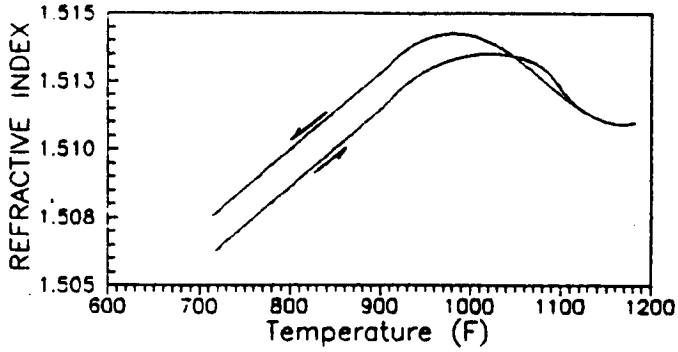

Figure 1c.

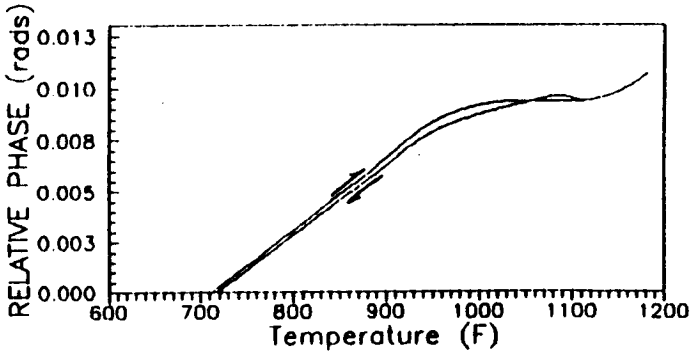

Figure 1d.

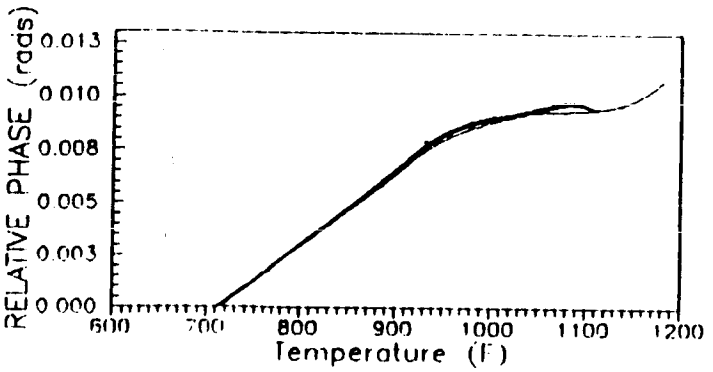

Figure 2.

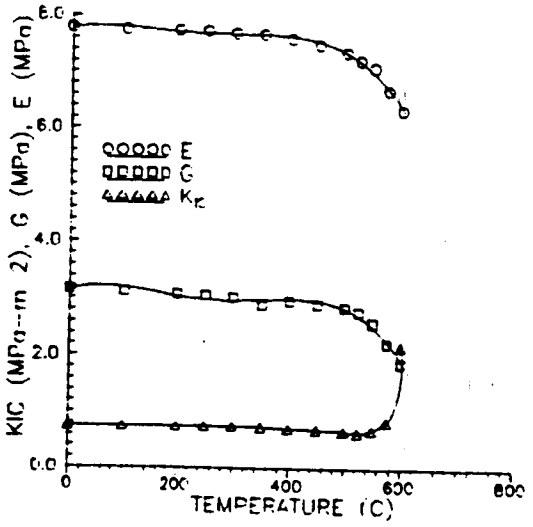

Figure 3.

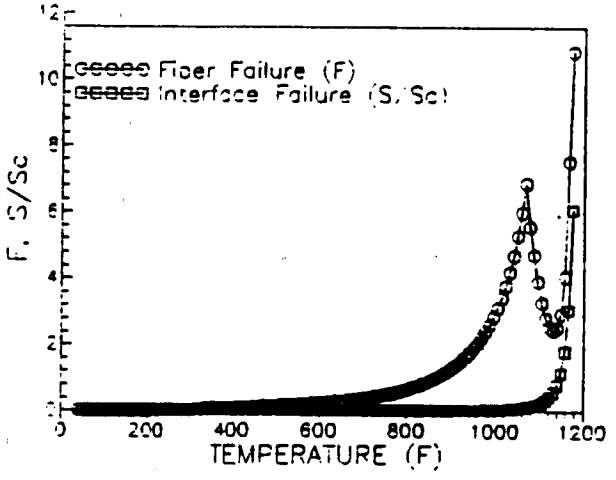

Figure 4.